of clay and organic matter, soil erodibility would decrease, and it increases by the increase of silt [29]. A group of researchers investigated the erodibility of soil in Talvarchai in Kordestan province and concluded that soil erodibility would increase by the increase of sand to silt ratio [30].

According to a researcher, the K factor is strongly correlated with soil loss and it is the key to predict the soil erosion [31]. Another researcher have argued that GIS tools used together with geostatistical models favour more realistic modeling, once the error related to the process has been attributed [32]. Knowledge of the spatial distribution of soil erodibility is the principal mechanism for implementing practices aimed at controlling erosion.

A previous researcher has argued that spatial investigation of soil physical properties is essential for understanding the spatial distribution of soil erodibility, a principal mechanism for implementig practices aimed to at controlling erosion [33]. In this way, geostatistics is emerging as an alternative for the prediction of spatial variability in different environments, with the correlation of soil erodibility. Geostatistics includes different methods that have increasingly used Kriging algorithms for estimating spatially continuous variables and spatial interpolation of values at unsampled locations, and it can be utilized for assessing spatial variability of K factor and distribution of soil properties [34-36].

The objectives of this study was based on: i) examining soils within El Hammam catchment to determine their erodibility factor (K) using alternative sources of soil sampling data; ii) evaluating and analyzing spatial variability of soil erodibility factor by using kriging model of geostatistics method and generating a spatial distribution map of soil erodibility, providing thus a more realistic means of evaluating spatial variability of K factor. This map associated with the soil physical properties could help to ascertain areas prone to erosion within the area of study.

2. MATERIALS AND METHODS

2.1 Study area

The El Hammam catchment is one of the sub-basins that constitute the Mellah catchment (550 km^2) and its main stream (El Hammam Wadi) is a tributary of the Seybouse River. It is located at the village of El Barnous, County of Hammam N'Bails (Figure 1).

The study catchment, with an area of 1000 Ha, has a Southwest - Northeast orientation. It drains the waters of the region of Douar Aine Ketoune. The use of the Digital Elevation Model (DEM) to generate the study catchment, with a spatial resolution of 30 m STRM, has shown that the elevation of El Hammam catchment is ranging from 346 to 1242 m. The El Hammam Wadi and its tributaries originate from hills such as Schvara Hills (864 m), Zouara Hills (1242 m), Bou Aichoun Hills (1102 m) and Besbessa Hills (963 m).
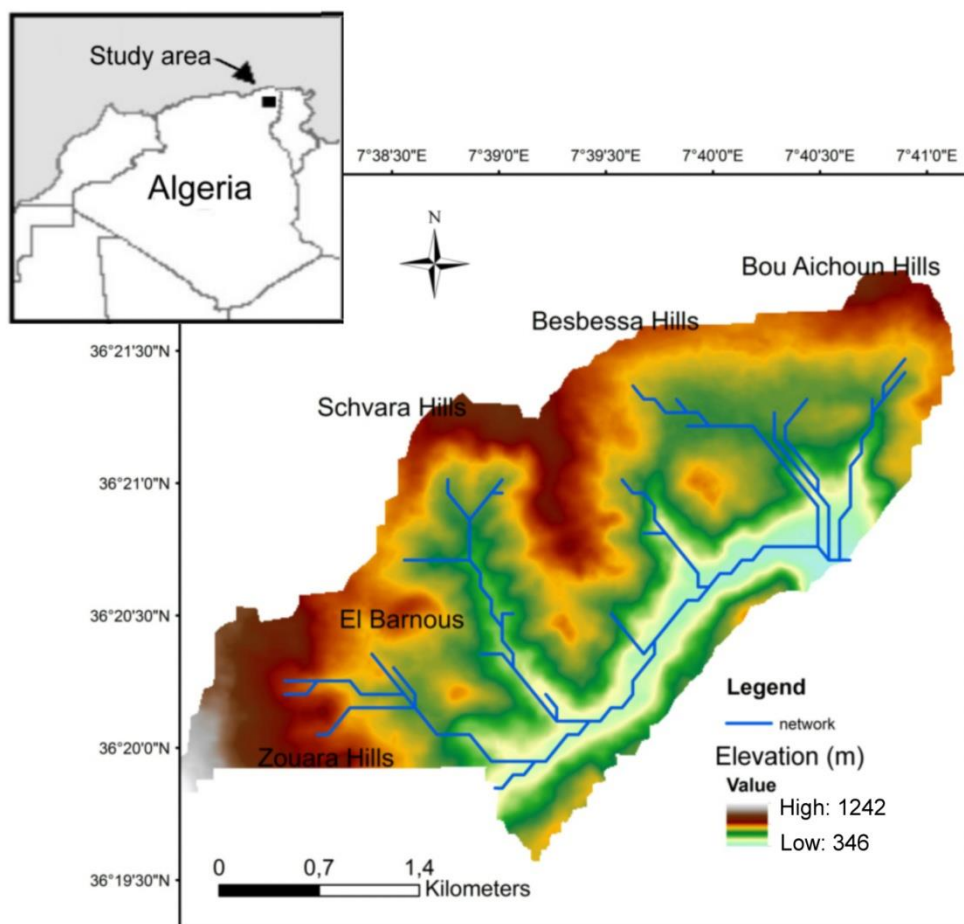
Figure 1: Map of the study area showing the elevation distribution

The study area is composed mainly of Mio-Pliocene weathered conglomerates with an area of 8.50 km^2 corresponding to 77% of the basin area. The northeastern part consists mainly of clay and Triassic gypsum with 8.00% and Cretaceous limestones with 7.50%, located in the South. The extreme southwest is composed of limestone and Upper Senonian marl (7.50%). The alluvium occupies the plain of Ch'Ramet wadi. The study basin is composed mainly of calcareous soils in association with Solonetz soil type [37].

The land use, which plays an important role in running water and soil erosion, is distinguished in the North-East part and the West part by large grasslands (63%). The North is occupied by crops (12.00%). The South has a sparsely forested area (16%) composed mainly of cork oak. The center of the basin consists of uncultivated land (3%). In the East, there are dense shrubs such as Oleo-mastic species (6%).

The basin is subject to a subhumid Mediterranean climate, which is part of the extreme north-east of Algeria, and shows a relatively well-watered

region of North Africa. The average annual rainfall from 1995 to 2016 is equal to 535mm. The study area is very wet during the autumn and winter periods. The spatial nuance of precipitation is likely to result in differential water erosion from year to year and from season to season within the same watershed.

2.2 Soil sampling and analysis

A field survey was been conducted to analyze the soil properties and study the soil erodibility status in the proposed catchment area. A systematic random technique was used for field sampling during April–May 2018. Grid sampling in addition to transect sampling have been done with grid size of 450m×550m. A total of 51 sample locations were identified to collect the soil samples. A Garmin portable GPS was employed in the field to collect the spatial location from each soil sample site (Figure 2). Disturbed and undisturbed soil samples were taken from a depth of 0 - 20 cm. For the undisturbed samples, a Uhland auger was used and the disturbed samples were collected with the aid of a hoe.
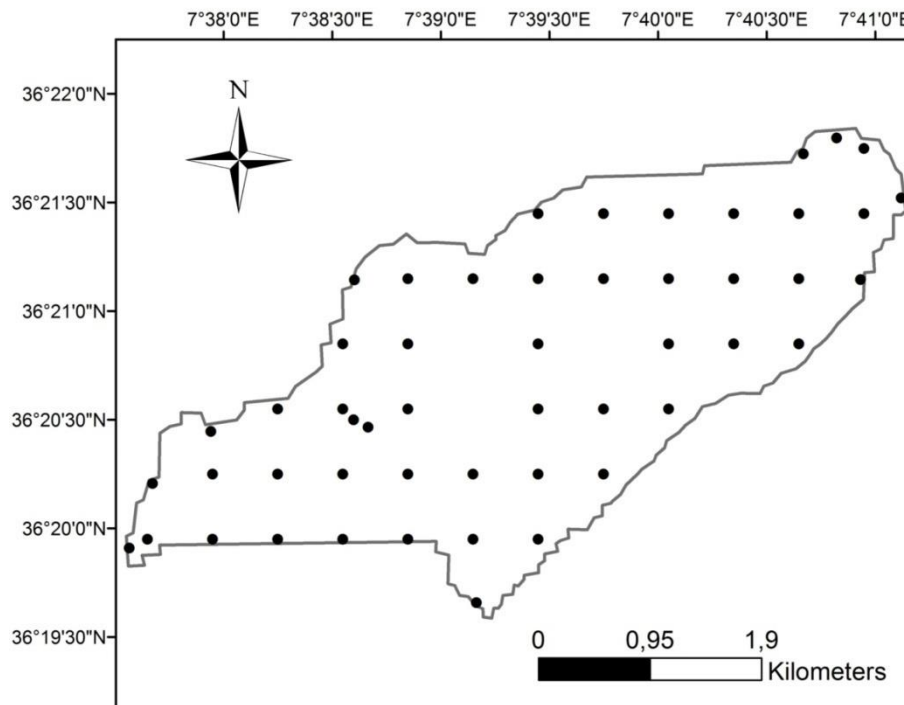
Figure 2: Soil sampling locations in the study catchment

The physical analysis of soil has been determined in the Soils and Sustainable Development Laboratory of the University of Annaba. The collected soil samples were taken to the laboratory, dried naturally and sieved with a 2mm sieve. The Robinson's pipette method was used for particles less than 20 μm. The size classes of soil particles in this study were based on USDA classes and were as follows: sand (0.005–2.0mm), silt (0.002–0.05mm), and clay (<0.002mm) [38]. Organic carbon was quantified by the Walkley–Black method (dichromate oxidation) and converted to organic matter by multiplying it by 1.724.

Soil permeability code was determined from the National Soils Handbook [39] and soil structure code was obtained using Soil Textural Pyramid [39-41]. To calculate soil erodibility, the formula of a researcher was used as [42]:

$$100K = 2.173 \times 2.1 \times M^{1.14} \times (10^{-4}) \times (12 - a) + 3.25 \times (b - 2) + 2.5 \times (c - 3) \tag{1}$$

Where:

K = soil erodibility (t·ha·h·ha^{-1}·Mj^{-1}· mm^{-1}), M = particles percentage (% of very fine sand + % of silt * (100 - %clay), a = organic matter content (% C * 1.724), b = soil structure code (very fine granular: 1-2mm; fine granular: 2-5mm; medium or coarse granular: 5-10mm; blocky, platy or massive: >10 mm), c = permeability code (c = 1, high to very high (>12.5cm/h); c = 2, moderate to high (6.25-12.5cm/h); c = 3, moderate (2-6.25cm/h); c = 4, low to moderate (0.5-2cm/h); c = 5, low (0.125-0.5cm/h); c = 6, very low (<0.125cm/h).

2.3 Geostatistical analysis

Geostatistics is based on spatial correlation between observations and this correlation can be expressed with a mathematical model which is called "variogram". Semivariogram, which is defined as half a variogram, was calculated to examine the spatial correlation within the measured data points. Geostatistical methods were employed to comprehend soil erodibility and its association with geomorphic conditions. Spatial inconsistency was estimated as a semivariogram which portrayed the mean square variability between the two neighbouring sample locations of distance h as shown in Eq. (2) [43]:

$$\gamma(h) = \frac{1}{2} \sum_{i=1}^{n} [Z(x_i + h) - Z(x_i)]^2 \tag{2}$$

Where (x_i) and (x_i+h) are sampling locations separated by a distance h. $Z(x_i)$ and $Z(x_i + h)$ are measured values of the variable Z at the corresponding locations. The experimental semivariogram $\gamma(h)$ is fitted with a theoretical model, such as spherical, exponential, linear, or Gaussian to determine three parameters, such as the nugget (c_0), the sill (c), and the range (r).

By programming Equation (2) we could compute the experimental variogram from data. The result depends on the precise way we apply the program and the decisions we make, that could be discussed after modelling [44]. The experimental variogram consists of semi variances at a finite set of discrete lags, whereas the underlying function is continuous for all h. The fitted smooth curve to the experimental values must have a mathematical expression that can describe the variances of random processes with changing lag and guarantee non-negative variances in the obtained predictions.

When calculating the experienced variogram, fitting a theoretical model is necessary to generalization of deduction and estimation of variables in points where they have not been sampled [45]. In the next spatial interpolation and spatial map creation of K factor, the kriging method was used. In this analysis an ordinary kriging was used because the mathematical expectation of the regionalized variable Z*(x) was unknown. Also, it is considered as one of the most accurate interpolation techniques which assumes that variables close in space tend to be more similar than those further away [46].

During calculation of experimental semivariogram values, maximum separation distance was fixed as half of the extent of the sampling area. The calculated experimental semivariogram values could be then fitted in the spherical during weighted least square fitting and defined by the following equation (3):

$$\gamma(h) = c_0 + c\left\{\frac{3h}{2r} - \frac{1}{2}\left(\frac{h}{r}\right)^3\right\} \text{ for } 0 < h \leq r$$
$$= c_0 + c \text{ for } h > r$$
$$= 0 \text{ for } h = 0, \tag{3}$$

In which h = |h| is the lag distance, and the parameters are c_0, the nugget variance, c the spatially correlated variance (sill variance), and r the range of distance parameter, which is the limit of spatial correlation. The quantity, $c_0 + c$, estimates the variance of the random process and is known as the 'partial sill'. The nugget variance, c_0, represents the uncorrelated variation at the scale of sampling; it is the variation that remains unresolved including any measurement error. The quantity c is the correlated component of the variation that represents continuity.

One of the major issues in variographic analysis is the selection of total lag distance for variogram fitting to experimental data [47]. For example, if the lag size is too large, short range autocorrelation may be masked. If the lag size is too small, there may be many empty bins, and sample sizes within bins will be too small to get representative averages for bins. The separation distance is selected based on the criterion that 95% pairs should have been used for variogram model fitting. The effect of removing data pairs at larger separation distance significantly might improve variogram model fitting to the soil erodibility data of El Hammam catchment.

The predictive performance of the fitted model was also checked by using ggplot function in R software package, contour plot of prediction of erodibility factor (K) has been depicted as it should be shown latter together with plot of standard error variance. The standard error (SE) of the estimate (usually an estimate of a parameter) is defined as the standard deviation of its sampling distribution or an estimate of that standard deviation. It is the standard deviation divided by the square root of the sample size.

2.4 Statistical analysis

Data were subjected to classical analysis using Gstat-R package to obtain descriptive statistics, namely the mean, minimum and maximum, standard deviation (SD), coefficient of variation (CV), and skewness of each parameter. Skewness is the most common statistical parameter to identify a normal distribution that is confirmed with skewness values varying from −1 to +1. A logarithmic transformation is considered where the coefficient of skewness is greater than 1. Prior to using geostatistics to obtain prediction maps, a preliminary analysis of data was done to check data normality. The normality of each dataset was checked by Kolmogorov–Smirnov test to ensure normal distribution, using XLSTAT 2018 program. The goodness of fit test was performed in order to test the following hypotheses: H_0 (null hypothesis): The K factor data follow the normal distribution; and H_1: the K factor data do not follow the specified distribution. The hypothesis regarding the distributional form is rejected

if the test statistic, D, is greater than the critical value obtained from a table [48].

The optimal fitting would be chosen on the basis of the cross-validation procedure, which checks the compatibility between the data and the structural model. In order to assess the accuracy of the model determined in theoretical variograms, parameters such as mean error (ME), root mean squared error (RMSE), index of spatial dependence (SPD) by a researcher, were calculated taking into account the observed and estimated values [49]. The performance measures were calculated considering the following equations:

$$ME = \frac{1}{n}\sum_{i=1}^{n}[Z(x_i) - Z^*(x_i)] \tag{4}$$

$$RMSE = \sqrt{\frac{1}{n}\sum_{i=1}^{n}[Z(x_i) - Z^*(x_i)]^2} \tag{5}$$

$$SPD(\%) = \left(\frac{C_1}{C_0 + C_1}\right) \times 100 \tag{6}$$

Where $Z(x_i)$ is the observed value at location i. $Z^*(x_i)$ is the predicted value at location i, and n is the sample size. Squaring the difference at any point gives an indication of the magnitude of differences, in such a way that a value of RMSE close to zero illustrates the accuracy of prediction of the model. It is assumed that if the variogram model is correct, ME should be almost zero [50]. Also, C_0 is the nugget effect and C_1 is the contribution. Adjusting the classification given by a scholar, the following induced SPD classification was explained by: weak spatial dependence (SPD (%) ≤ 25 %), moderate spatial dependence (25 % < SPD (%) ≤ 75 %), and strong spatial dependence (SPD (%) > 75 %) [51].

3. RESULTS

3.1 Descriptive statistics of soil properties and erodibility

Basic statistical parameters of the soil properties for the topsoil (0–20 cm) layers are listed in Table 1. The mean content of sand in the topsoil (28.06%) was slightly lower and that of silt (42.03%) slightly higher, whereas the clay content was equal to 29.91%. Mean organic matter (OM) in the topsoil layer was 3.45%.

As indicated by the coefficient of variation (CV), the largest variations were exhibited by the clay content (53.04%), intermediate – the sand content (48.91%), and the lowest – the silt content (27.56%). The organic matter was much more variable (63.14%). In addition, the soil erodibility factor (K) has shown a mean value of 0.36 and CV of 38.82%. According to the classification proposed by Dahiya et al. [52], CV values were medium (15-75%) for all the soil properties (sand, clay, silt, and organic matter).

Table 1: Summary statistics for content of soil textural fractions. soil organic matter content (OM).

Parameter	Sand (%)	Clay (%)	Silt (%)	OM (%)	K
Minimum	5.80	7.52	16.88	0.10	0.16
Maximum	59.60	63.52	65.88	9.01	0.66
Mean	28.06	29.91	42.03	3.45	0.36
Standard deviation	13.73	15.86	11.58	2.18	0.14
Coefficient of variation	48.91	53.04	27.56	63.14	38.82
Skewness	0.51	0.53	0.01	0.92	0.42
Kurtosis	2.66	2.49	2.21	3.27	2.06

The skewness for a normal distribution is zero, and any symmetric data should have skewness near zero. Negative values for the skewness indicate data that are skewed left and positive values for the skewness indicate data that are skewed right [53]. Moreover, the kurtosis for a standard normal distribution is three. Positive kurtosis indicates a

"peaked" distribution and negative kurtosis indicates a "flat" distribution [53].

Distribution of soil properties, except the silt content, and K factor were positively skewed, indicating moderate to high values in this area of El

Hammam (0.42-0.92). Meanwhile, the silt content has the lowest skewness, indicating a normal distribution of the data. The organic matter and sand contents had the highest positive kurtosis value, indicating a "peaked" distribution. Nevertheless, the application of the Kolmogorov and Smirnov test has indicated that all the K erodibility data were normally distributed. It was found that D calculated (D = 0.103) was greater than the critical value (here D critical = 0.19 or p-value of 0.62) at the 0.05 significance level, the hypothesis on the distributional form could not be rejected.

3.2 Relationships between K factor and soil properties

Table 2 has presented Pearson correlation coefficients (r) between the soil parameters and soil erodibility factor at $p < 0.05$. In table 2, K factor was significantly and negatively correlated with the topsoil clay content and soil permeability (−0.72 and −0.64) and positively correlated with the silt and sand contents and soil structure (0.48, 0.42, 0.21). Topsoil organic matter was significantly and negatively correlated with K factor.

Table 2: Correlation coefficients (r) between soil variables and erodibility factor.

| Variables	Clay	Silt	Sand	OM	Perm.	Struc.	K
Clay	1.00						
Silt	-0.54	1.00					
Sand	-0.70	-0.22	1.00				
OM	0.00	-0.04	0.03	1.00			
Perm	0.93	-0.42	-0.72	0.06	1.00		
Struc	0.08	0.06	-0.14	-0.17	0.15	1.00	
K	-0.72	0.48	0.42	-0.48	-0.64	0.21	1.00

Perm.: Soil permeability; Struc.: soil structure

It seems from the soil permeability classification, mentioned in the previous section, that 39.22% of the basin soils have moderate permeability (class 3) corresponding mainly to loam silt, loam; followed by 23.53% of soils having moderate to low permeability (class 4) and indicating a texture of sandy clay loam, clay. The soils of very low permeability have occupied 19.61% and they were composed of silty clay, clay. Nevertheless, in most cases soil permeability and K-factor have correlated significantly with the amount of loam, sandy clay, clay and organic matter. Concerning the soil structure, as shown in Table 2, it has low relationships with the other soil properties and K factor. The study basin has shown 31.37% of soils with very fine granular structure (class 1). These soils might represent a texture of fine sand and silt greater than 50%. The rest of soil structures have been varying from coarse granular (25% of area) to fine granular - compact or massive structure (22% of area).

3.3 Geostatistical analysis

The distributions of the measurement data were similar to the normal distribution and thus have met the condition of a stationary or quasi stationary process in geostatistical analysis with the exception of the clay and organic matter contents in the topsoil layer [54]. Nevertheless, K factor has shown a good normal distribution. The spherical model well matched the empirical semivariogram data for all quantities of K.

The spatial dependency "nugget-to-sill" for the K factor was strong (<25%). The nugget effect did exist in the chosen spherical model. The greatest value for the sill was equal to 0.0204 for the K factor (Figure 3). The effective range of the spatial dependence for the latter parameter has a value of 703.71 m.
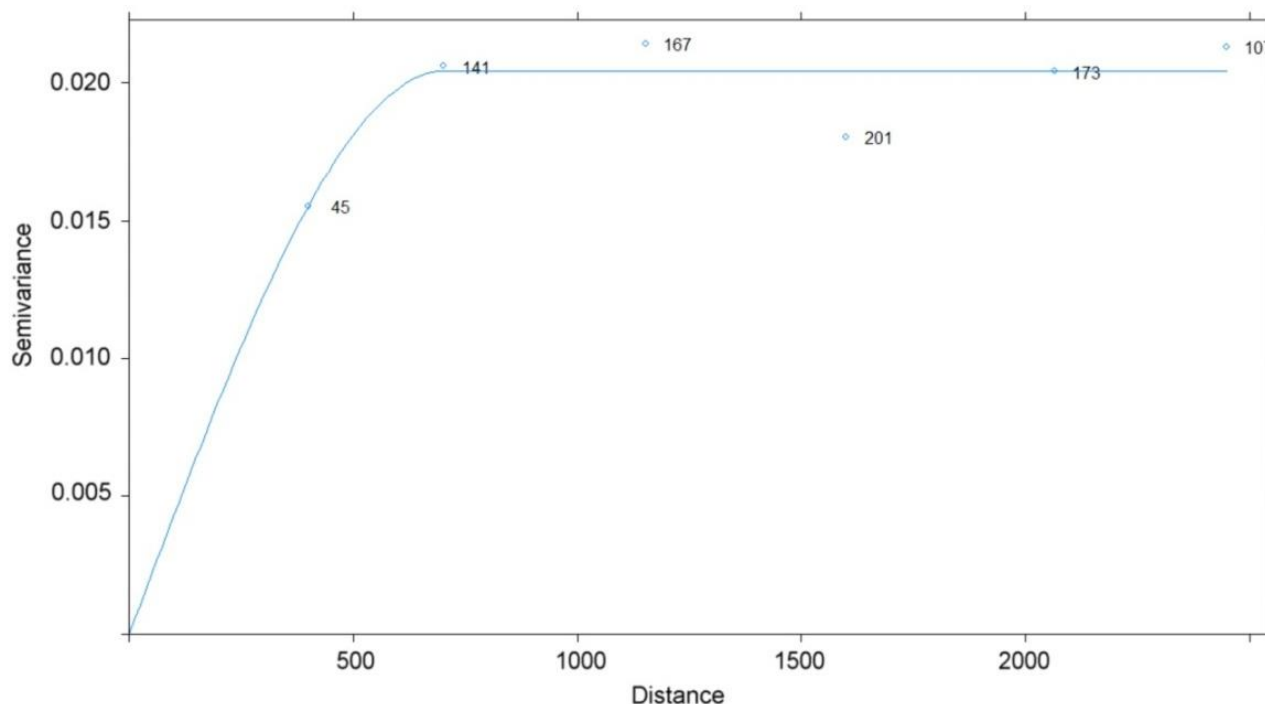
Figure 3: Semivariogram of K factor

Cross-validation facilitated the selection of the best-fit semivariogram for an interpolation K map, which could provide the most accurate prediction. Closer values of the ME and RMSE to 0, suggested that the prediction values were close to measured values. The K model was best fitted with a spherical model, and the statistical values, such as ME with 4.042e^{-05} and RMSE having a value of 0.00162, have given a good semivariogram pattern that was well fitted with the observed data at a lag size equivalent to 460m.

4.DISCUSSION

This study has provided information on how K factor were correlated and spatially dependent on selected soil physical properties. The discussion has focused on the spatial pattern of the soil erodibility factor and in a way the context of sustainable field management to raise and line up the yields on the different soil types.

4.1 Correlation analysis

In general, the Pearson correlation coefficients between the studied soil properties and K factor were rather moderate to fairly high (Table 2). This was related to the fact that erodibility El Hammam conditions were a resultant of both positive and negative effects of soil factors, weather conditions, and different spatial distribution patterns of soil properties and morphogenic processes. The highest negative and significant correlations in this study were obtained for clay soils and permeability, which were -0.72 and -0.64. This might indicate that a reduction of clay content in the soil might increase soil erosion; leading to a critical decrease of particle cohesion in soil.

Laboratory and visual observations of the field carried out by the authors have indicated no excessively wet periods that could induce insufficient aeration (oxygen stress) occurred on the highly permeable soil. Hence, the negative relationship between the K factor and soil permeability relative to the excess of silt content could result mostly from low excessive penetration of water in denser soils. It is known that the content silt + very fine sand lacks adhesion properties and it can be moisturized, this content becomes easily broken and transported, leading to an increased impact on soil erodibility.

The value for organic matter, of 3.45% in this class of soil, has reduced the erodibility value but not by enough to alter its classification of high erodibility (mean value of 0.36) (Table 1). The dataset of organic matter has shown that almost 65% of the OM content had soil organic carbon (SOC) less than 2%, which could explain that soil aggregates were considered unstable; meanwhile, only 24% of SOC content had soil aggregates very stable (SOC > 2.5%) [55]. Consequently, increasing the amount of organic matters in soil protect aggregates from disintegration in such a way that by considerable increase of organic matters, disintegration of the aggregates could be reduced. Also, the presence of organic and clay coatings usually increases soil aggregate stability, hence soil degradation and erodibility [56]. Moreover, the soil erodibility increase with samples from croplands has higher values of susceptibility as a result of their high sandy content. Sandy soils are known to have low cohesive force and are prone to detachment and transportation by water

and wind. High sandy soil content encourages high rate of permeability of water into soil, which induces landslide and erosion [57].

Nevertheless, helpful conclusions regarding the relationship of the erodibility K factor to a specific soil property could be drawn from the study of particular components of the overall variables if all terms, that could involve different soil properties, were considered together as a single entity.

4.2 Geostatistical analysis and spatial distribution

The cross-validation results of the mean K value of the estimation of error (ME) was very low, i.e. close to zero, which has shown that a spherical can be estimated by the Kriging method. Also, the low value of the root mean square of error (RMSE) indicated that the estimation had an acceptable accuracy. Therefore, the results of the control semivariogram have shown the suitability of estimation by Kriging (Figure 3). Thus, these two statistical parameters previously analyzed have presented summarily the indicators which helped to choose the most appropriate model of semivariogram for the creation of a prediction K map. Also, the strong spatial dependency, due to the changes in intrinsic soil characteristics, was controlled by such elements as the soil texture and the soil type.

Gstat-R package was used to calculate the soil erodibility factor and create the spatial distribution map for the entire study area. The variability of spatial soil properties can be influenced by natural factors (such as particle-size composition and topography) and anthropogenic factors (such as land cover or management practices) [58]. The map of the spatial variation of K factor has shown that El Hammam catchment has relatively moderate erodibility that ranged from 0.17 to 0.28 t.ha.h.ha^{-1}.Mj^{-1}.mm^{-1} with a contribution of 24.50% (Figure 4a). Meanwhile, the severe and considerably severe soil erodibility levels were greater than 0.28 and included 75.41% of the basin area. These levels were considered poorly graded silt or fine sandy soil.

The general trend has shown that lower soil erodibility was mainly observed in western, southwestern and southern part and higher soil erodibility was predominant in the middle, western, extreme southwestern and southeastern parts, as shreds, in the study area (Figure 4a). The intensive cultivation triggered the dominance of silt particles and lack of SOM in the soil system. These intensive practices decreased OM in soils, making them poor and vulnerable to the soil erosion process. This eventually led to the aggravation of soil erosion. The eastern part of the basin is bestowed with sparse forest land. In fact, land use types played the most prominent role in determining the variation of soil properties and thereby dictated the risk of soil erosion.
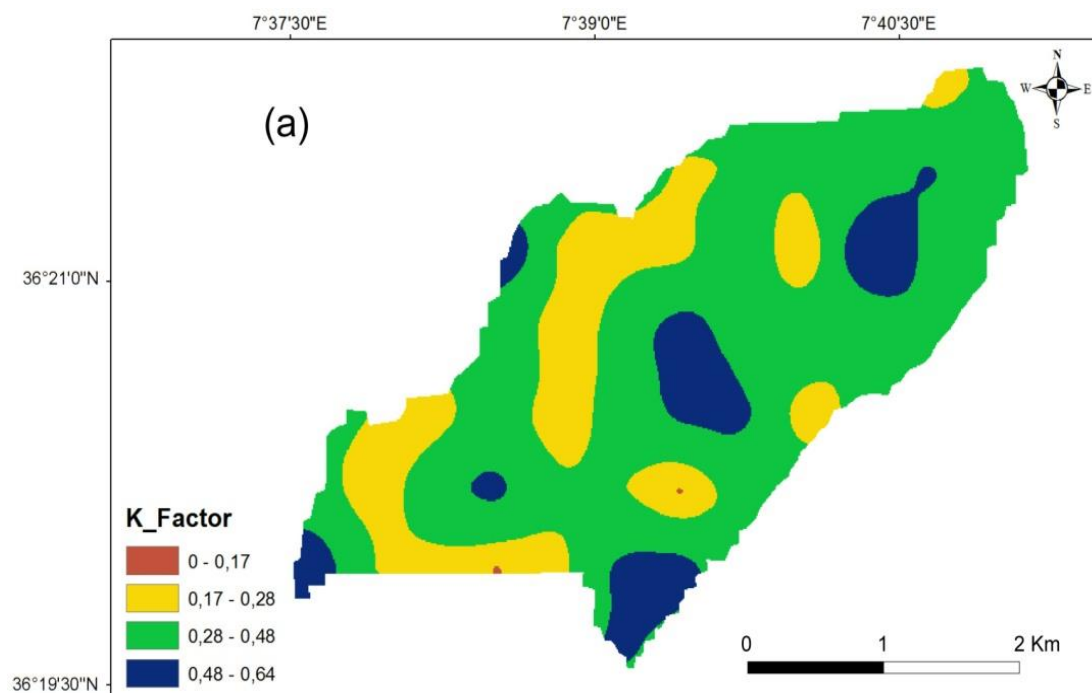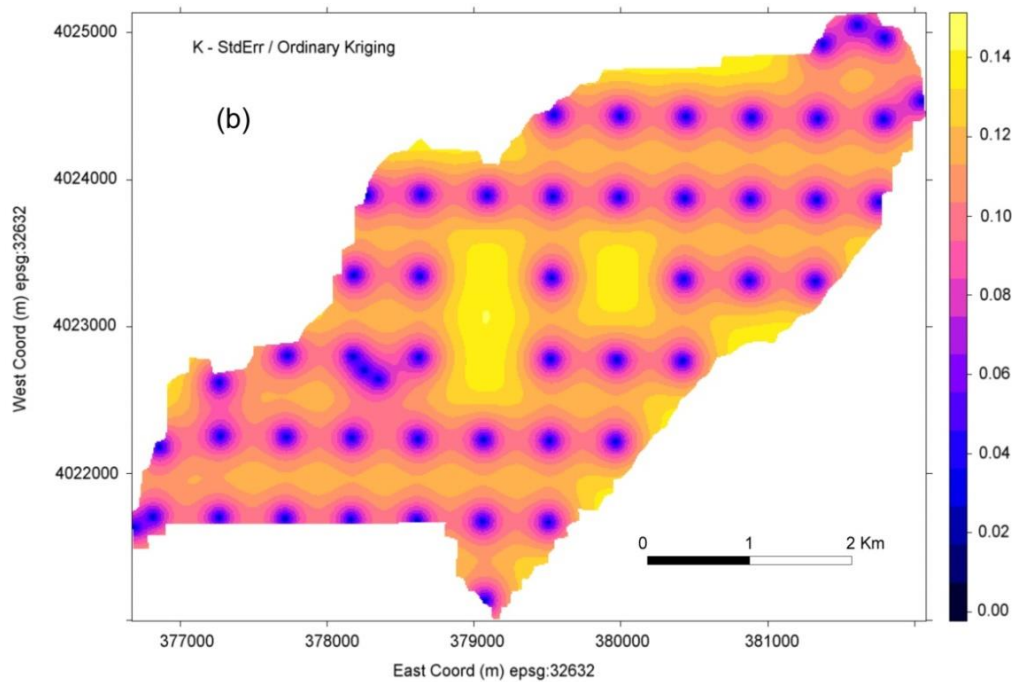
Figure 4: Soil erodibility map (a) and K standard error map (b) for El Hammam catchment.

Areas with severe erodibility in the basin have high amounts of silt and very fine sand, as a result, these soils tend to have moderate to low permeability and low resistance to particle detachment. El Hammam catchment is less rich on clay particles. It should be noted that these particles might be less susceptible to erosion than other types because of their ability to form stable aggregates. It is notable that in the study basin, despite being a clay soil in some parts of the basin, it has the influence of chemical properties that affect this property such as the high exchangeable Na+ percentage found in the the Solonetz soil, because it acts as an ion that disperses the soil particles. It is also responsible for separating organic matter particles of sand, silt and clay, causing poor structure in the soil [59].

To ascertain further reliability of the erodibility surface map developed by ordinary kriging, the standard error maps were also created (Figure 4b). The error map has indicated that the interpolated surface map to predict the spatial variation of soil erodibility was quite reliable and can be used for developmental purpose. It is northworthy to mention that higher error values were associated with the areas having low sampled point cloud and where higher potential erosion risk was expected.

5. CONCLUSION

The presented spatial soil erodibility map was an important contribution to the estimation of soil erosion from local to Algerian scales, as the K-factor was very crucial among the input factors used to estimate soil erosion level. In addition, the K-factor could usually not easily be determined by individual with no extensive data access. We have examined in this study soil erodibility factor at field scale and established relations between soil properties and erodibility. Statistical analysis in El Hammam basin has shown negative correlation of erodibility with clay and organic matter content. The effect of organic matter in reducing erodibility of the soil is due to its role in creation of aggregates and their stability. The predisposition of soil to erosion was found to be significantly dependent on silt content.

El Hammam catchment has shown K-values varying between 0.16 and 0.66 with a mean value of 0.36 and more than 50% of K-values exceeding 0.30. Soil erosion modelling is so complicated because many factors effects on spatial and temporal variability of soil losses. Results of the research area indicated kriging method was so useful to know the spatial distribution of soil erodibility factor. Thus, the proposed Ordinary Kriging model has provided a framework for the digital soil mapping of the soil erodibility at El Hammam catchment. Among the mostly used semivariogram models, the spherical model was the one which had the ability of zoning the variables of the study area with high accuracy and less

error. The range of the spatial variation of soil erodibility factor was 460m. Results of this research have revealed that the soil erodibility in this catchment was classified from moderate up to severe level. The estimated soil erodibility factor had the highest values, exceeding 0.28, spread all over the basin, while the lowest values of soil erodibility factor were observed as small and scattered parts. Soil texture, organic matter content, soil structure, and permeability have presented the soil properties that could influence the soil erodibility. However, the ability of clay particles to form stable aggregates that might oppose particle detachment could not reduce the potential soil erodibility because of its reduced content in the study area. In addition, erodibility values were derived solely from soil properties and did not consider factors such as slope, rainfall, land use or agricultural soil practices.

The spatial patterns of soil erodibility obtained from the semivariogram model were successfully acquired over the study area and quite reliable. It can have a significant implication in prediction of land degradation and help to define the location and the type of soil conservation practices to use through the catchment.

REFERENCES

[1] Fotouhi, F., Azimzadeh, H.R., Talebib, A., Ekhtesasic, M.R. 2012. Analyzing the changes of soil erodibility index (K) in the soils of arid regions and the effective factors in central Iran (case study: Yazd-Ardakan Plain). Desert, 17, 65-75.

[2] Pradeep, G.S., Ninu Krishnan, M.V., Vijith, H. 2015. Identification of critical soil erosion prone areas and annual average soil loss in an upland agricultural watershed of Western Ghats, using analytical hierarchy process (AHP) and RUSLE techniques. Arabian Journal of Geosciences, 8(6), 3697-3711.

[3] Borrelli, P., Robinson, D.A., Fleischer, L.R., Lugato, E., Ballabio, C., Alewell, C., Meusburger, K., Modugno, S., Schütt, B., Ferro, V., Bagarello, V., van Oost, K., Montanarella, L., Panagos, P. 2017. An assessment of the global impact of 21st century land use change on soil erosion. Nature Communications, 8(1). DOI.org/10.1038/s41467-017-02142-7

[4] Schmidt, S., Ballabio, C., Alewel,l C., Panagos, P., Meusburger, K. 2018. Filling the European blank spot—Swiss soil erodibility assessment with topsoil samples. Journal of Plant Nutrition and Soil Science, 181(5), 737-748.

[5] Marzen, M., Iserloh, T., de Lima, J., Fister, W., Ries, J.B. 2017. Impact of severe rain storms on soil erosion: Experimental evaluation of wind-

driven rain and its implications for natural hazard management. Science of the Total Environment, 590-591, 502-513.

[6]   Adhikary, P.P., Tiwari, S.P., Mandal, D., Lakaria, B.L., Madhu, M. 2014. Geospatial comparison of four models to predict soil erodibility in a semi-arid region of Central India. Environmental Earth Sciences, 72, 5049-5062.

[7]   Zhang, X., Zhao, W., Wang, L., Liu, Y., Feng, Q., Fang, X., Yue Liu, X. 2018. Distribution of shrubland and grassland soil erodibility on the Loess Plateau. International Journal of Environmental Research and Public Health, 15(6), 1193, 1-17.

[8]   Panagos, P., Meusburger, K., Ballabio, C., Borrelli, P., Alewell, C. 2014. Soil erodibility in Europe: A high-resolution dataset based on LUCAS. Science of the Total Environment, 479-480, 189-200.

[9]   Al Rammahi, A.H.J. 2018. Estimation of soil erodibility factor in Rusle equation for Euphrates River Watershed using Gis. International Journal of GEOMATE, 14, 164-169.

[10]   Saadoud, D., Guettouche, M.S., Hassani, M., Peinado, F.J.M. 2017. Modelling wind-erosion risk in the Laghouat region (Algeria) using geomatics approach. Arabian Journal of Geosciences, 10, 363. DOI.org/10.1007/s12517-017-3139-1

[11]   Kumar, S., Gupta, S. 2016. Geospatial approach in mapping soil erodibility using CartoDEM - A case study in hilly watershed of Lower Himalayan Range. Journal of Earth System Science, 125, 1463-1472.

[12]   Karmaker, T., Das, R. 2017. Estimation of riverbank soil erodibility parameters using genetic algorithm. Sādhanā, 42, 1953-1963.

[13]   Meshesha, D.T., Tsunekawa, A., Haregeweyn, N. 2016. Determination of soil erodibility using fluid energy method and measurement of the eroded mass. Geoderma, 284, 13-21.

[14]   Wei, H., Zhao, W.W., Wang, J. 2017a. Research process on soil erodibility. Chinese Journal of Applied Ecology, 28, 2749-2759.

[15]   Ayoubi, S., Mokhtari, J., Mosaddeghi, M.R., Zeraatpisheh, M. 2018. Erodibility of calcareous soils as influenced by land use and intrinsic soil properties in a semiarid region of central Iran. Environment Monitoring and Assessment, 190, 192. DOI: 10.1007/s10661-018-6557-y

[16]   Larionov, A.G., Bushueva, O.G., Gorobets, A.V., Dobrovolskaya, N.G., Kiryukhina, Z.P., Krasnov, S.F., Litvin, L.F., Maksimova, I.A., Sudnitsyn, I.I. 2018. Experimental study of factors affecting soil erodibility. Eurasian Soil Science, 51, 336-344.

[17]   Mahalder, B., Schwartz, J.S., Palomino, A.M., Zirkle, J. 2018. Relationships between physical-geochemical soil properties and erodibility of streambanks among different physiographic provinces of Tennessee, USA. Earth Surface Processes and Landforms, 43, 401-416.

[18]   Belasri, A., Lakhouili, A., Iben Halima, O. 2017. Soil erodibility mapping and its correlation with soil properties of Oued El Makhazine watershed, Morocco. Journal of Materials and Environmental Sciences, 8(9), 3208-3215.

[19]   Wang, B., Zheng, F., Guan, Y. 2016. Improved USLE-K factor prediction: a case study on water erosion areas in China. International Soil and Water Conservation Research, 4,168-76.

[20]   Thomas, J., Joseph, S., Thrivikramji, K.P. 2018. Assessment of soil erosion in a tropical mountain river basin of the southern Western Ghats, India using RUSLE and GIS. Geoscience Frontiers, 9, 893-906.

[21]   Bronstert, A., De Araújo, J.C., Batalla, R.J., Vericat, D. 2014. Process-based modelling of erosion, sediment transport and reservoir siltation in mesoscale semi-arid catchments. Journal of Soils and Sediments, 14, 2001-2018.

[22]   Cordeiro, M.R.C., Lelyk, G., Kröbel, R., Legesse, G., Faramarzi, M., Masud, M.B, McAllister, T. 2018. Deriving a dataset for agriculturally relevant soils from the soil landscapes of Canada (SLC) database for use in Soil and Water Assessment Tool (SWAT) simulations. Earth System Science Data, 10, 1673-1686.

[23]   Hajigholizadeh, M., Melesse, A.M., Fuentes, H.R. 2018. Erosion and sediment transport modelling in shallow waters: A review on approaches, models and applications. International Journal of Environmental Research and Public Health, 15(3), 518, 1-24.

[24]   Cassol, E.A., Silva, T.S., Eltz F.L.F., Levien, R. 2018. Soil erodibility under natural rainfall conditions as the K factor of the universal soil loss equation and application of the nomograph for a subtropical Ultisol. Revista Brasileira de Sciencia do Solo, 42, e0170262.

[25]   Wang, L., Qian, J., Qi, W.Y., Li, S.S., Chen, J.L. 2018. Changes in soil erosion and sediment transport based on the RUSLE model in Zhifanggou watershed, China. Proceedings of the International Association of Hydrological Sciences, 377, 9-18.

[26]   Wischmeier, W.H., Johnson, C.B., Cross, B.V. 1971. A Soil erodibility nomogram for farmland and construction sites. Journal of Soil and Water Conservation, 26, 189-193.

[27]   Loch, R.J., Slater, B.K., Devoil, C. 1998. Soil erodibility (Km) values for some Australian soils. Australian Journal of Soil Research, 36, 1045-1055.

[28]   Charman, P.E.V., Murphy, B.W. 2000. Soils (their properties and management). Second edition. Land and Water Conservation, New South Wales, Oxford, 206-212.

[29]   Ghasemi A., Mohammadi, J. 2003.Study of spatial variation of soil erodibility. A case study in Cheghakhor watershed in Chaharmahal-e-Bakhtiyari province. Proceeding of the Eighth Soil Science Congress of Iran (In Persian), Rasht., Iran, 864-865.

[30]   Ghaderi, N., Ghoddosi, J. 2005. Study of soil erodibility in lands units from Telvarchai watershed. Proceedings of the Third National Conference of Erosion and Sediment (In Persian), Tehran, Iran, 367-372.

[31]   Imani, R., Ghasemieh, H., Mirzavand M. 2014. Determining and mapping soil erodibility factor (case study: Yamchi Watershed in northwest of Iran). Open Journal of Soil Science, 4, 168-173.

[32]   Saygin, S.D., Ozcan, A.U., Basaran, M., Timur, O.B., Dolarslan, M., Yilman, F.E., Erpu, G. 2014. The combined RUSLE/SDR approach integrated with GIS and geostatistics to estimate annual sediment flux rates in the semi-Arid catchment, Turkey. Environmental Earth Sciences, 71, 1605-1618.

[33]   Addis, H.K., Klik, A. 2015. Predicting the spatial distribution of soil erodibility factor using USLE nomograph in an agricultural watershed, Ethiopia. International Soil and Water Conservation Research, 3, 282-290.

[34]   Li, J., Heap, A.D. 2008. A review of spatial interpolation methods for environmental scientists. Geoscience Australia, Record 2008/23, 137.

[35]   Pereira, E.C.B., Lopes, F.B., Gomes, F.E.F., de Almeida, A.M.M., de Magalhães, A.C.M., de Andrade, E.M. 2017. Determining the soil erodibility for an experimental basin in the semi-arid region using geoprocessing. American Journal of Plant Sciences, 8, 3174-3188.

[36]   Yin, S., Zhu, Z., Wang, L., Liu, B., Xie, Y., Wang, G., Li, Y. 2018. Regional soil erosion assessment based on a sample survey and geostatistics. Hydrology and Earth System Sciences, 22, 1695-1712.

[37]   Service Géographique de l'Algérie. 1948. Carte des sols d'Algérie. Feuille de Constantine, N.J.32.S.O.

[38]   Wang, D.C., Zhang, G.L., Pan, X.Z., Zhao, Y.G., Zhao, M. S., Wang, G.F. 2012. Mapping soil texture of a plain area using fuzzy-c-means clustering method based on land surface diurnal temperature difference. Pedosphere, 22(3), 394-403.

[39]   USDA. 1983. National Soil Survey Handbook. US Department of Agriculture, N° 430, USDA, Washington DC.

[40]   Wischmeier, W.H., Smith, D.D. 1979. Predicting rainfall erosion losses-A guide to conservation planning. Predicting rainfall erosion losses. A guide to conservation planning, 1-57.

[41]   Hashim, G.M., Wan Abdullah, W.Y. 2005. Prediction of soil and nutrient losses in a highland catchment. Water, Air and Soil Pollution, 5, 103-113.

[42]   Wischmeier, W.H., Smith, D.D. 1978. Predicting rainfall erosion losses, a guide to conservation planning. U.S. Department of Agriculture, Agricultural Handbook, 537, 58.

[43]   Bhunia, G.S., Shit, P.K., Chattopadhyay, R. 2018. Assessment of spatial variability of soil properties using geostatistical approach of lateritic soil (West Bengal. India). Annals of Agrarian Science, 16, 436-443.

[44]   Oliver, M.A., Webster, R. 2014. A tutorial guide to geostatistics: computing and modelling variograms and kriging. Catena, 113, 56-69.

[45]   Kavianpoor, H., Esmali Ouri, A., Jafarian Jeloudar, Z., Kavian, A. 2012. Spatial variability of some chemical and physical soil properties in Nesho Mountainous Rangelands. American Journal of Environmental Engineering, 2(1), 34-44.

[46]   Goovaerts, P. 1999. Geostatistics in soil science: State-of-the-art and perspectives. Geoderma, 89(1-2), 1-45.

[47]   Lakhankar, T., Jones, A.S., Combs, C.L., Sengupta, M., Vonder Haar, T.H., Khanbilvardi, R. 2010. Analysis of large scale spatial variability of soil moisture using a geostatistical method. Sensors, 10(1), 913-932.

[48]   Ghosh, S., Roy, M.K., Biswas, S.C. 2016. Determination of the best fit probability distribution for monthly rainfall data in Bangladesh. American Journal of Mathematics and Statistics, 6(4), 170-174.

[49]   Biondi, F., Myers, D.E., Avery, C.C. 1994. Geostatistically modeling stem size and increment in an old-growth forest. Canadian Journal of Forest Research, 24(7), 1354-1368.

[50]   Wackernagel, H. 1995. Multivariate geostatistics: an introduction with applications. Springer, Berlin.

[51]   Cambardella, C.A., Moorman, T.B., Novak, J.M., Parkin, T.B., Karlen, D.L., Turco R.F., Konopka, A.E. 1994. Field-scale variability of soil properties in Central Iowa soils. Soil Science Society of America Journal, 58(5), 1501-1511.

[52]   Dahiya, I.S., Richter, J., Malik, R.S. 1984. Soil spatial variability: a review. International Journal of Tropical Agriculture, 2, 1-102.

[53]   Hosking, J.R.M. 2006. On the characterization of distributions by their LL-moments. Journal of Statistical Planning and Inference, 136(1), 193-198.

[54]   Usowicz, B., Lipiec, J. 2017. Spatial variability of soil properties and cereal yield in a cultivated field on sandy soil. Soil and Tillage Research, 174, 241-250.

[55]   Greenland, D.J., Rimmer, D., Payne, D. 1975. Determination of the structural stability class of English and Welsh soils, using a water coherence test. European Journal of Soil Science, 6(3), 294-303.

[56]   Mazllom, U., Emami, H., Haghnia, G.H. 2016. Prediction the soil erodibility and sediments load using soil attributes. Eurasian Journal of Soil Science, 5(3), 201-208.

[57]   Peter, A.I., Mustapha, H.I., Musa J.J., Dike J. 2008. Determination of erodibility indices of soils in Owerri West Local Government Area of Imo State, Nigeria. Assumption University Journal of Technology, 12(2), 130-133.

[58]   Tesfahunegn, G.B., Tamene, L., Vlek, P.L.G. 2011. Catchment-scale spatial variability of soil properties and implications on site-specific soil management in northern Ethiopia. Soil and Tillage Research, 117, 124-139.

[59]   Sposito, G.1989. The Chemistry of Soils. Oxford University Press, New York, 277.